

Lawrence Berkeley National Laboratory

Recent Work

Title

Impedance studies of the LiMn₂O₄/LiPF₆-DMC-EC interface

Permalink

<https://escholarship.org/uc/item/5bp71522>

Author

Cairns, Elton J.

Publication Date

2000-11-08

IMPEDANCE BEHAVIOR OF THE $\text{LiMn}_2\text{O}_4/\text{LiPF}_6\text{-DMC-EC}$ INTERFACE DURING CYCLING

Kathryn Striebel, Eiji Sakai and Elton Cairns
Environmental Energy Technologies Division
Ernest Orlando Lawrence Berkeley National Laboratory,
Berkeley, California 94720 USA

ABSTRACT

Room temperature impedance measurements of the $\text{LiMn}_2\text{O}_4/\text{LiPF}_6\text{-EC-DMC}$ interface have been used to identify a previously unreported step in the formation of the SEI layer on this cathode. The low frequency impedance and potential of pure dense LiMn_2O_4 films was found to depend logarithmically on time in the end-of-discharge (EOD) state. The rate of the impedance rise decreased with Mn^{3+} content. The increased impedance was removed by oxidation of the film to 4.5 V vs. Li/Li^+ . The observations are consistent with a reversible disproportionation of part of the LiMn_2O_4 into $\text{Li}_2\text{Mn}_2\text{O}_4$ and $\lambda\text{-Mn}_2\text{O}_4$. Analyses of cyclic voltammograms and impedance spectra at intervals during constant current cycling of the LiMn_2O_4 films suggest that $\text{Li}_2\text{Mn}_2\text{O}_4$ on the surface also plays a major role in the capacity fade.

INTRODUCTION

The stability of the interface between LiMn_2O_4 and LiPF_6 -containing carbonate electrolytes, especially at elevated temperature, is critical to the commercial application of this battery system. Degradation products have been reported to form as a mostly inorganic layer at this interface at temperatures around 55°C ¹, however positive identification of the mechanism of the degradation remains elusive, since most studies focus on bulk analysis tools such as XRD^{1,2} and highly degraded electrodes. In our lab we have been using thin dense films of LiMn_2O_4 , produced with pulsed laser deposition, as a model system for the study of the electrochemical properties of this important cathode material^{3,4}. Recently we have employed electrochemical impedance spectroscopy (EIS) to the study of the oxide/electrolyte interface focusing first on the basic impedance behavior of LiMn_2O_4 films as a function of state-of-charge (SOC) and time⁵. In this paper, a mechanism for the first step in the formation of the SEI layer on this oxide is proposed on the basis of impedance and cyclic voltammetry measurements. In addition, impedance changes during the current cycling of these films are discussed.

EXPERIMENTAL

Pure LiMn_2O_4 films are crystalline as prepared by pulsed laser deposition (PLD), at 600°C and 100 mtorr O_2 , on polished ($0.1\ \mu\text{m}$) $0.3\ \text{cm}^2$ -diameter stainless steel substrates. Their structure, morphology and electrochemical behavior have already been reported^{3,4}. Films are studied by embedding the 3 mm disk into the end of a polypropylene rod, which is inserted into a polypropylene cell, fitted with lithium reference and counter electrodes and filled with about 5 ml of 1M $\text{LiPF}_6/\text{EC}/\text{DMC}$ (1:2) electrolyte (EM Science). Elevated temperature measurements are carried out with this cell by heating the walls with cartridge-heaters and an on-off controller optimized for low noise operation. However, impedance measurements were recorded with the heater power turned off. During the measurements, the temperature of the electrolyte dropped by a few degrees over the length of the experiment. Cyclic voltammetry (1 mV/s), used for film characterization, was carried out with a PAR 273 potentiostat. Electrochemical Impedance Spectroscopic (EIS) measurements were carried out with a Solartron 1260 FRA and a Solartron 1286 potentiostat using a perturbation of $\pm 10\text{mV}$ between 80k and 60mHz controlled by the ZPlot software. EIS data were fit to various circuit models with the ZView software.

RESULTS

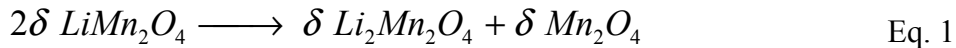
The LiMn_2O_4 films were crystalline as prepared with lattice parameters very near $8.24\ \text{\AA}$, suggesting that they are close to stoichiometric. Lithium content was not measured directly due to the small chemical inventory of the PLD films, however, it has been shown to be dependent on the target-substrate distance. Film capacity was measured with slow-sweep cyclic voltammetry (CV) and the thickness was estimated using a theoretical density of $4.4\text{g}/\text{cm}^3$. The films reported here had capacity densities of $12\text{-}15\ \mu\text{Ah}/\text{cm}^2$ and were nominally $0.3\ \mu\text{m}$ thick. In general, the LiMn_2O_4 films prepared in our lab show electrochemical behavior very similar to those of bulk powders, however without the need for binders or conductive diluents. However, they tend to show somewhat better cycling stability, probably due to the lower stresses associated with a 2-dimensional geometry.

Reversible Film Formation at the Surface

The shape of the first CV recorded for fresh LiMn_2O_4 films immersed in electrolyte at room temperature was always quite different from the steady shape observed after three cycles between 3.7 and 4.5 vs. Li/Li^+ . Originally this behavior was attributed to a disorder of the lithium within the Mn_2O_4 framework deposited by PLD. However the first CV shape was found to depend strongly on the time elapsed between immersion and the first measurement. This behavior was characterized extensively with EIS⁵, since direct current measurements altered the response of the film. The impedance at end-of-discharge (EOD) conditions was found to increase logarithmically with time. The impedance at end-of-

charge (EOC) was independent of time for up to several days. Fig.1 shows the time dependence of the total impedance at a fixed frequency, near the top of the main interfacial loop, for two different films under several different conditions. Curves 1 and 2 are for fresh films measured at EOD and a mid-SOC, respectively. These impedance rises were accompanied by logarithmic increases in the open-circuit potential of the film. The reversible nature of this behavior was observed with cyclic voltammetry. The first anodic sweep after an 18 h period for a discharged film (EOD) was considerably distorted with peak potentials shifting about 80 mV anodically and the two original peaks tending to collapse into a single peak. The distorted shape was quite similar to that observed for the first CV recorded on a fresh film (see Fig.2). And as for the fresh film, the original steady-state CV was retraced after 3 cycles between 3.7 and 4.5 vs. Li/Li⁺. No film capacity fade was recorded after a one day hold at open circuit for either charged or discharged films, suggesting that neither Mn nor Li was lost.

Voltage rises at EOD have been observed previously with thin film electrodes⁶ at elevated temperatures and have been attributed to a disproportionation ($2\text{Mn}^{3+} \rightarrow \text{Mn}^{2+} + \text{Mn}^{4+}$) followed by Mn²⁺ dissolution in LiPF₆/carbonate electrolytes, leaving the higher voltage λ -MnO₂. However, this process is not reversible and the degradation of the LiMn₂O₄ will result. We believe that we are observing an initial step in this process. At room temperature the disproportionation reaction proceeds as far as the formation of Li₂Mn₂O₄ on the surface according to the reaction



Li₂Mn₂O₄ is a known insulator, which would lead to a high-impedance surface layer. The λ -MnO₂ phase would cause the observed increase in the open-circuit voltage of the film. In addition, Li₂Mn₂O₄ is expected to be oxidized upon cycling to 4.5 V vs. Li/Li⁺. It might be argued that Li₂Mn₂O₄ is not expected to be present at potentials above 3 vs. Li/Li⁺. We have observed oxidation peaks in the same potential region for LiMn₂O₄ films reduced well into the tetragonal phase region with CV, also shown in Fig. 2. These peaks were explained as the slow removal of Li⁺ from the octahedral sites, that are populated in the tetragonally-distorted spinel³. Some characteristics of the Li₂Mn₂O₄ phase have been observed with Raman spectroscopy of SEI layers in these electrolytes⁷. Spectroscopic analysis of the surface films will be investigated further. Limited measurements of the impedance behavior of these films at elevated temperatures have been carried out (see Fig. 1) on a well-cycled discharged film that suggest that increasing the temperature does not accelerate the rate of Li₂Mn₂O₄, although more data are obviously needed to characterize the temperature dependence of the surface reaction.

Cycling Studies

EIS was also investigated as a tool to examine changes in the behavior of LiMn_2O_4 films with constant-current cycling. The formation of the $\text{Li}_2\text{Mn}_2\text{O}_4$ layer on the film with time was the same before and after cycling, also shown in Fig. 1, however the starting impedance was clearly higher after cycling. To gain insight into the changes occurring within the film as well as at the interface during cycling, cyclic voltammograms and impedance spectra as a function of state-of-charge were measured at different points during the cycling. Films were cycled at $\pm 10\mu\text{A}/\text{cm}^2$ (about 2.3C) between 3.7 and 4.35 V. Initially we used 15 min. open circuit rest periods between half cycles (regimen A). However, because of the large impedance increases at EOD discussed above, the cycling regimen was modified to include only 15 s rest periods (regimen B). In general, the change in cycling protocol did not improve the capacity retention with cycling. However, there was a clear difference in the pattern of the material loss after cycling with the different regimens. Figure 3 shows CV's recorded before and after cycling with the two regimens. In both cases the loss in capacity was about 12% but the shapes of the CV's was quite different. For regimen B, the CV suggests that the film thickness is simply decreased with cycling. For regimen A, with significant time spent at EOD during the cycling (18% of each cycle) the current signal is more dispersed in voltage and the separation between the anodic and cathodic peaks is increased. This behavior is characteristic of an increase in the film porosity and the formation of a resistive layer, respectively. EIS was used to investigate this further.

Sample Nyquist plots measured for a LiMn_2O_4 film before and after cycling with regimen B are shown in Fig. 4. Impedance changes with time, SOC and cycle history are manifested in the frequency range of 200 Hz to 60mHz. These spectra along with those recorded at intermediate SOC's (not shown) were modeled with the circuit shown in Fig. 5. Spectra recorded for films cycled with regimen A are visibly the same as those in Fig. 4, however, the circuit model had to be modified by replacing the capacitor C_1 with an additional constant-phase element. It should be noted that spectra were recorded by charging the film to a given SOC and then holding for 15 min at OC before making the measurement. These data will necessarily be complex to interpret since the $\text{Li}_2\text{Mn}_2\text{O}_4$ on the surface at each SOC will be different and dependent on the total elapsed time as well as the direction of the measurements. An effort was made to automate the measurements with the Batch mode in the Zplot software so they were carried out in the same fashion each time.

There are nine parameters that result from the circuit in Fig.5. The changes in all of the parameters with SOC and cycling are summarized in Table 1, along with suggested explanations for the observed dependencies. At a given SOC, the formation of $\text{Li}_2\text{Mn}_2\text{O}_4$ was correlated with a logarithmic increase in the charge-transfer resistance, R_{ct} . The rate of increase slowed with a decrease in the Mn^{3+} in the film (see Fig. 1). At a fixed time, both film interfacial resistance and R_{ct} were affected, suggesting that the $\text{Li}_2\text{Mn}_2\text{O}_4$ formation affects both the interfacial resistance and the kinetics of lithium insertion. R_{ct} was also found to increase with cycling at all SOC. Since the rate of $\text{Li}_2\text{Mn}_2\text{O}_4$ formation was found to be the same on fresh and cycled films (Fig. 1), there must be another mechanism acting as well. The Warburg element is thought to characterize the diffusion process within the film and $W_T=L^2/D$ where L is the thickness of the film. Therefore,

increases in W_T with SOC should be characteristic of decreased Li^+ -diffusivity in LiMn_2O_4 at lower lithium contents. Decreases in W_T and increases in the CPE_P parameter (characteristic of the depression of the center of the loop below the real axis) probably reflect decreases in the film thickness and an increases in film porosity with cycling, respectively.

Table 1. Circuit Parameter Changes with SOC and Cycling

Parameter	Change with Cycling		Change with \uparrow SOC	
R_s	\downarrow	less film, less ohmic resistance	NC	OK
R_1	NC	v. small change	$\downarrow\downarrow$	less $\text{Li}_2\text{Mn}_2\text{O}_4$ formed
C_1	\uparrow	Incr. In porosity?	NC	OK
R_{ct}	\uparrow	OK	\downarrow	less $\text{Li}_2\text{Mn}_2\text{O}_4$
CPE_P	\downarrow	\uparrow porosity/roughness	NC	OK
CPE_T	\uparrow	?	NC	OK
W_T	\downarrow	\downarrow Film thickness	\uparrow	\downarrow Li^+ mobility
W_P	\uparrow	?	$\uparrow\downarrow$	OK
W_R	\uparrow	?	$\uparrow\downarrow$?

CONCLUSIONS

The room temperature impedance response of thin dense LiMn_2O_4 films was used to investigate the formation of the SEI layer on this oxide as well as mechanism of oxide degradation during cycling in LiPF_6 -containing electrolyte. The impedance rise with time at 3.7 volts is consistent with a reversible disproportionation reaction of part of the LiMn_2O_4 into $\text{Li}_2\text{Mn}_2\text{O}_4$ and λ - Mn_2O_4 at the surface. The CV and EIS analysis of these films during cycling suggests that this step is involved with the degradation of the LiMn_2O_4 film.

ACKNOWLEDGMENTS

We would like to thank R. Reade for the preparation of the films, T. Richardson for discussions and R. Kesticki for the Raman studies. This work was supported by the Office of Energy Research, Basic Energy Sciences, Chemical Sciences Division of the Department of Energy under contract No. DE-ACO3-76SF00098.

REFERENCES

1. A. Du Pasquier, A. Blyr, P. Courjal, D. Larcher, G. Amatucci, B. Gerand and J-M. Tarascon, *J. Electrochem. Soc.* **146**, 428 (1999).
2. J. Cho and M.M. Thackeray, *J. Electrochem. Soc.* **146** (1999) 3577.
3. A. Rougier, K.A. Striebel, S. J. Wen, T.J. Richardson R.P Reade and E.J. Cairns, *Appl. Surf. Sci.* **134**, 107 (1998).

4. K.A. Striebel, A. Rougier, C.R. Horne, R.P. Reade and E.J. Cairns, *J. Electrochem. Soc.*, **146**, 4339 (1999).
5. K.A. Striebel, E. Sakai and E.J. Cairns, submitted to *Rechargeable Lithium Batteries*, K.M. Abraham, E.S. Takeuchi and M. Doyle, eds, PV2000, The Electrochem. Soc. Meeting, Phoenix, AZ, Fall 2000.
6. T. Uchiyama, M. Nishizawa, T. Itoh and I. Uchida, *J. Electrochem. Soc.* **147**, 2057 (2000).
7. R. Kosteki, personal communication, Dec. 2000.

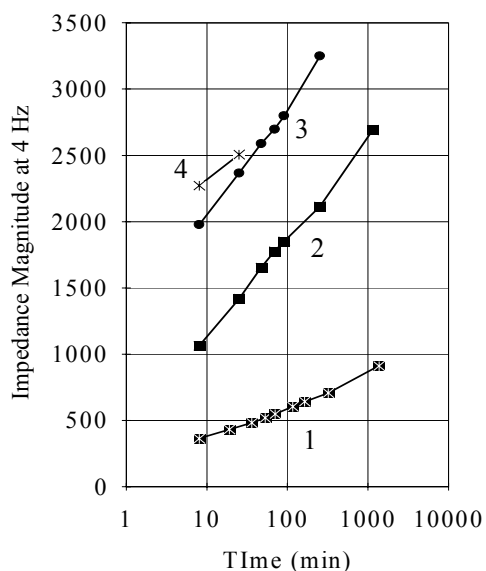


Figure 1. $|Z|$ at 4 Hz for films in 1M $\text{LiPF}_6/\text{EC}/\text{DMC}$ (1:2): 1: fresh film at mid-SOC, 2: fresh film at EOD, 3: cycled film at EOD and 4: cycled film at EOD and 55°C .

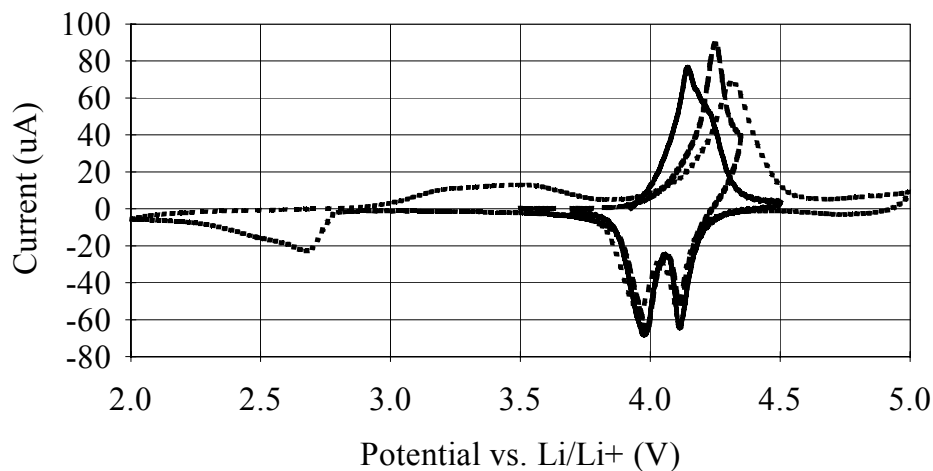


Figure 2. Comparison of anodic peak voltages for different cathodic treatments: ●●● sweep down to 2 V, — — 1 h hold @ 3.5V, ——— 18h hold at 3.7 V.

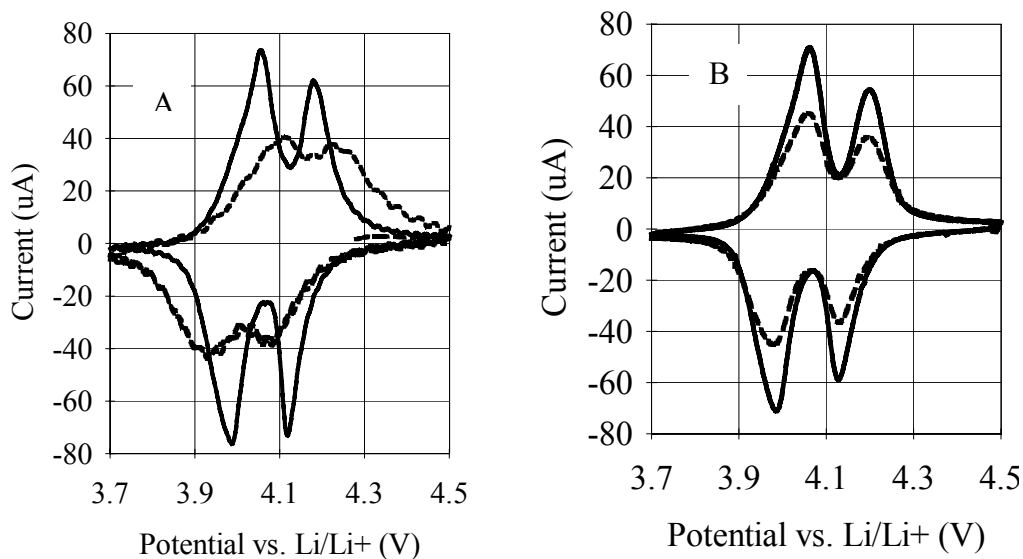


Figure 3. Comparison of CV change with different cycling protocols: LiMn_2O_4 films cycled at constant current ($\pm 10\mu\text{A}$) with (A) and without (B) 15 min. OC periods between half-cycles.

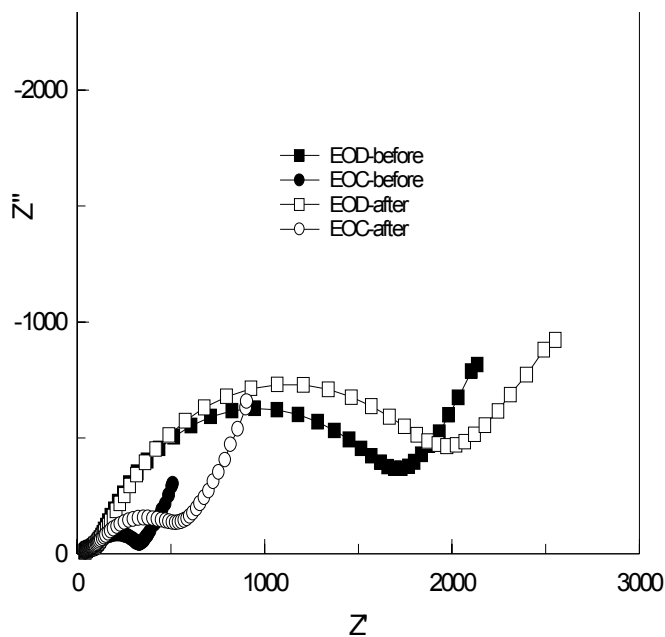


Figure 4. Nyquist plots for a LiMn_2O_4 film at EOD and EOC, before and after 88 cycles.

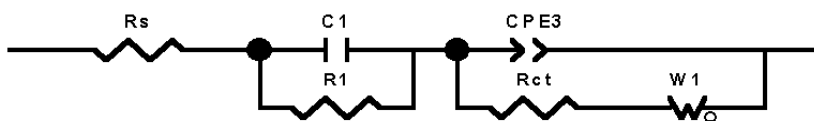


Figure 5. Circuit for modeling impedance data from LiMn_2O_4 film on stainless steel.